THE JOURNAL OF
PHYSICAL CHEMISTRY C

Article

pubs.acs.org/JPCC

Exploring the Real Ground-State Structures of Molybdenum Dinitride

Shuyin Yu,*[,†,‡] Bowen Huang,[§] Xiaojing Jia,[†] Qingfeng Zeng,[†,‡] Artem R. Oganov,[‡,∥,⊥,#] Litong Zhang,[†] and Gilles Frapper*[,§]

[†]Science and Technology on Thermostructural Composite Materials Laboratory, School of Materials Science and Engineering, Northwestern Polytechnical University, Xi'an, Shaanxi 710072, China

[‡]International Center for Materials Discovery, School of Materials Science and Engineering, Northwestern Polytechnical University, Xi'an, Shaanxi 710072, China

[§]IC2MP UMR 7285, Université de Poitiers - CNRS, 4, rue Michel Brunet TSA 51106−86073 Poitiers Cedex 9, France

[∥]Skolkovo Institute of Science and Technology, 3 Nobel Street, Skolkovo 143025, Russia

[⊥]Department of Geosciences, Center for Materials by Design, and Institute for Advanced Computational Science, State University of New York, Stony Brook, New York 11794-2100, United States

[#]Moscow Institute of Physics and Technology, Dolgoprudny, Moscow Region 141700, Russia

S *Supporting Information*

ABSTRACT: Molybdenum dinitride (MoN_2) was recently synthesized at a moderate pressure of 3.5 GPa, and a layered MoS_2-type structure has been proposed. However, our first-principles calculations of thermodynamic, mechanical and dynamical properties suggest that this layered *R*3*m* structure is unstable. Therefore, stable structures of MoN_2 at pressures from atmospheric pressure to 100 GPa have been further examined by utilizing a widely adopted evolutionary methodology USPEX for crystal structure prediction. We find that the ground state of the MoN_2 system is a pernitride structure with space group $P6_3/mmc$ which transforms to a *P*4/*mbm* phase above 82 GPa. Chemical bonding analysis shows that one could assign MoN_2 as $Mo^{4+}(N_2^{4-})$; i.e., Mo is formally a d^2 metal, in agreement with the experimental results of Wang et al. The presence of covalent N_2 dumbbells and strong bonding between Mo^{4+} and N_2^{4-} is the source of the superior mechanical properties of these predicted ultra-incompressible MoN_2 pernitrides.

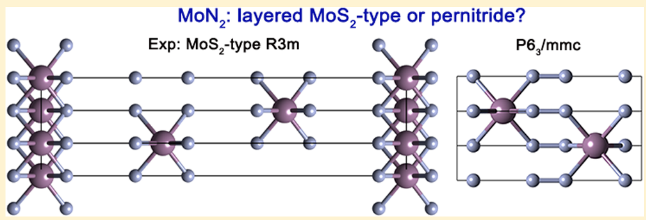

1. INTRODUCTION

Nearly a century since the pioneering works in the 1920s−1930s by G. Hägg in crystal structure determination of transition metal nitrides M_xN_y (M, transition metal such as Fe[1] and Mo[2]), the elucidation of the atomic arrangement in binary metal−nitrogen phases is still a delicate task. Many MN_{1-z} in the literature are possibly oxynitrides, imides, or amides; thus, efforts have to be made to assign a valid crystal structure for a given stoichiometry.[3] The understanding of their peculiar mechanical and chemical properties, such as high stiffness, high hardness, high thermal conductivity, high melting point,[4] and good catalytic performance,[5,6] needs characterization of materials from a crystallographic point of view. Their fascinating properties stimulate the development of new synthetic routes leading to new well-defined nitride materials.

Most of the 1:1 and substoichiometric MN_{1-z} structures contain single nitrogen atoms (formally nitride N^{3-}) encapsulated in a metallic network.[7] A number of studies in the Zr−N,[8] Hf−N,[8,9] Ta−N,[10,11] and W−N[12] systems have demonstrated the power of high-pressure synthesis in the search for new nitrogen-rich nitrides. The entire field of synthesis and study of the high oxidation state of transition metal nitrides has been reviewed recently by Salamat et al.[13]

Recently, a novel family has emerged in which the content of nitrogen exceeds the metal content, namely, MN_2. These phases have been successfully synthesized at extreme conditions (P = 11−50 GPa and T > 2000 K) with M = Pt,[14,15] Pd,[16] Ir,[14,17] Os,[17] and recently Ru.[18,19] If one considers a metal oxidation number lower than 6, two N^{3-} may not be assigned in such MN_2 phases. Thus, one may expect from simple electron counting that covalent N−N bonds should form. This is what we see in all synthesized or predicted nitrogen-rich MN_2 phases, possessing diatomic N_2 units, and such MN_2 materials should be called pernitrides.

In 2015, a nitrogen-rich molybdenum-based compound, MoN_2, was proposed by Wang et al.,[20] extending the well-known binary Mo−N compositions. This newly discovered nitride, 3R-MoN_2, adopts a rhombohedral *R*3*m* structure, and was proposed to be isotypical with MoS_2. This structure is a bulk layered material in which the layers interact via van der Waals forces (Figure 1a). Mo is located in a trigonal prismatic atomic arrangement and sandwiched between N atoms. The

Received: January 21, 2016
Revised: April 28, 2016
Published: April 29, 2016

DOI: 10.1021/acs.jpcc.6b00665
J. Phys. Chem. C 2016, 120, 11060−11067

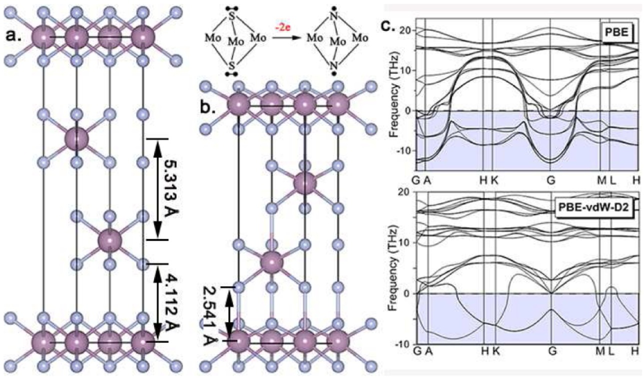

Figure 1. (a) Experimental claimed MoS_2-type $R3m$ MoN_2 and formal electron attribution on tricoordinated X atoms in MoX_2 (X = S, N; Mo^{4+}, d^2). (b) Fully optimized $R3m$ crystal structure at the PBE vdW-D2 level. (c) The associated phonon dispersion curves of the fully relaxed $R3m$ structure with/without van der Waals correction.

"determined valence state for Mo is +3.5 in both 3R-MoN_2 and MoS_2" claimed by Wang et al.,[20] to our astonishment as MoN_2 has two valence electrons less per formula unit than in MoS_2. Therefore, nitrogen atoms do not fulfill the octet rule in the proposed $R3m$ MoN_2, as sulfur does in MoS_2 (Figure 1a, see the formal electron attribution on tricoordinated X atoms in MoX_2 (X = S, N; Mo^{4+}, d^2)). We hypothesized that this electronic situation should be very unstable from thermodynamic and mechanical points of view and that adjacent MoN_2 layers must be connected through N−N covalent bonding, leading to the well-known pernitride situation (diatomic N_2 units in Mo network).

There are at least two questions that needed to be answered: first, what is the ground-state structure of MoN_2? Knowledge of solid-state MoN_2 geometrical and electronic properties is crucial for understanding the catalytic properties of such a nitrogen-rich molybdenum phase.[21] Second, as the synthesis of MN_2 is done under moderate or high pressure, what is the effect of pressure on solid-state MoN_2? To address these issues, the crystal structures of MoN_2 were explored by the *ab* initio evolutionary crystal structure prediction method (USPEX). New ground states and metastable MoN_2 structures at both ambient and high pressures are proposed and established. The previously proposed $R3m$ MoN_2 is found to be thermodynamically, dynamically, and mechanically unstable, while a pernitride phase ($P6_3/mmc$) emerges as the ground-state structure. We systematically investigated their elastic and thermodynamic stabilities, XRD spectra, and chemical bonding, which would provide theoretical guidance for the experimental structural redetermination of MoN_2.

2. COMPUTATIONAL DETAILS

The search for thermodynamically stable MoN_2 structures was performed using the evolutionary algorithm, as implemented in the USPEX code.[22−24] The lowest-energy structures were determined at 0, 10, 20, 40, and 100 GPa with systems containing up to six formula units (f.u.) in the simulation cell. The first generation of 100 structures was produced randomly; all subsequent generations contained 80 structures and were produced using variation operators such as heredity (60%), softmutation (15%), lattice mutation (15%), and 10% of each new generation was produced randomly. To update a full-scale Mo−N phase diagram, variable-composition structure predictions were also performed at 0 and 40 GPa to search for thermodynamically stable Mo_xN_y structures.

Each structure was fully relaxed to an energy minimum at different pressures within the framework of density functional theory by using the VASP package.[25] We employed the all-electron projector-augmented wave (PAW) method and the Perdew−Burke−Ernzerhof (PBE)[26] version of the generalized gradient approximation (GGA) functional. The PAW potentials have [Kr] and [He] cores with radii of 2.30 and 1.50 a.u. for Mo and N atoms, respectively. A plane-wave basis set with a kinetic energy cutoff of 600 eV was employed. We used uniform Γ-centered k-point meshes with a reciprocal space resolution of $2\pi \times 0.03$ Å^{-1} for Brillouin zone sampling. These settings enable excellent convergence of total energies, forces, and stress tensors.

Theoretical phonon spectra were calculated on the basis of the supercell approach by using the PHONOPY package[27] in order to probe the dynamical stability of the enthalpically preferred Mo−N structures. The calculated phonon dispersion curves are given in the Supporting Information. All discussed energies are zero-point energy (ZPE) corrected. Note that, if any phonons of a given structure exhibit imaginary frequencies, the studied structure is dynamically unstable and should transform under lattice relaxation into a more stable ground state structure. The elastic tensors were further calculated for all dynamically stable structures, and the mechanical stabilities were determined by Born−Huang criteria.[28] Chemical bonding analyses were carried out by means of the crystal orbital Hamilton population (COHP) method[29] by using the LOBSTER code.[30,31]

3. RESULTS AND DISCUSSION

3.1. Experimental Layered *R3m* MoN_2 Structure. In the experimentally claimed layered 3R-MoN_2 structure displayed in Figure 1a, each MoN_2 sheet consists of a hexagonally packed molybdenum layer sandwiched between two nitrogen layers. The optimized crystallographic parameters are given in Table 1.

Table 1. Calculated Structural Parameters for MoN_2 Phases at Selected Pressures (Å, GPa)

phase	P	lattice parameter	atom coordinates
$R3m$ unrelaxed	0	a = 2.854	Mo (0, 0, 0)
		c = 15.938	N (0, 0, 0.258)
			N (0, 0, 0.402)
$R3m$ PBE	0	a = 3.012	Mo (0, 0, 0)
		c = 13.869	N (0, 0, 0.253)
			N (0, 0, 0.411)
$R3m$ vdW-D2	0	a = 3.119	Mo (0, 0, 0)
		c = 11.214	N (0, 0, 0.235)
			N (0, 0, 0.416)
$P6_3/mmc$ PBE	0	a = 2.927	Mo (0.333, 0.667, 0.75)
		c = 7.762	N (0, 0, 0.089)
$P4/mbm$ PBE	100	a = 4.077	Mo (0.5, 0.5, 0.5)
		c = 2.597	N (0.385, 0.885, 0)

The calculated Mo−Mo bond length is 3.012 Å, slightly longer than that found in bulk fcc Mo (2.729 Å) at ambient pressure. Mo atoms are positioned in a trigonal prismatic coordination with respect to the two nitrogen layers. Each Mo atom is coordinated by six N atoms at distances of 2.044/2.062 Å (exp. 1.976/2.037 Å). Moreover, within the $R3m$ space group, the fully optimized structure—both lattice and atomic positions—

DOI: 10.1021/acs.jpcc.6b00665
J. Phys. Chem. C 2016, 120, 11060−11067

Table 2. Calculated Elastic Constants C_{ij}, Bulk Modulus B, Shear Modulus G, Young's Modulus E, Poisson's Ratio υ, κ = G/B Ratio, and Vickers Hardness H_v of MoN_2 Phases at Ambient Pressure (All in GPa, Except Dimensionless G/B Ratio)

phase	C_{11}	C_{12}	C_{13}	C_{14}	C_{33}	C_{44}	C_{66}	B	G	E	υ	κ	H_v
*R*3*m*	230	144	39	41	14	−222	43						
$P6_3/mmc$	516	185	201	0	952	216	165	338	206	514	0.247	0.61	22.3
*P*4/*mbm*	690	184	155	0	740	234	251	345	251	607	0.207	0.73	32.0

presents a dramatic decrease of the van der Waals region. The *c* lattice parameter goes from 15.939 (exp. value, magnetic phase) to 13.869 Å (opt. value, nonmagnetic phase, Table S1), reducing the interlayer Mo−N separation down to 3.256 Å.

While the 2D MoS_2-like MoN_2 layer is magnetic as expected[32] (Table S1), the coupling of unpaired electrons localized on two adjacent layers is responsible for the ferromagnetic to nonmagnetic phase transition. However, the state-of-the-art DFT is not a suitable method for studying interactions in loosely packed systems (such as soft matter, van der Waals complexes, and biomolecules), as this method fails to adequately describe the long-ranged dispersion interactions.[33,34] Therefore, we performed a full structural optimization by using the PBE-GGA DFT level and vdW-D2 method of Grimme[35] for van der Waals correction (Table 1). The structural parameters within the covalent 2D MoN_2 sheet are very similar, while the lattice constant *c* decreased from 13.869 Å (PBE without vdW correction) to 11.214 Å (PBE with vdW-D2 correction). Therefore, short interlayer Mo−N contacts appear (Mo−N = 2.541 Å) and *R*3*m* is no more a MoS_2-like layered structure (Figure 1b). This phenomenon illustrates the strong structural instability of the claimed layered MoS_2-type *R*3*m* MoN_2 structure.

To ensure whether such a MoS_2-type structure is a stable local minimum on the MoN_2 potential energy surface, we have examined its mechanical and dynamical stabilities by calculating the elastic constants and phonon spectrum. *R*3*m* is found to be mechanically unstable due to the negative C_{44} value of −222 GPa (Table 2), and large imaginary frequencies are found over the entire Brillouin zone (Figure 1c). When van der Waals correction is taken into account, the fully relaxed *R*3*m* structure is also found to be dynamically unstable with very large imaginary frequencies (Figure 1c). One may conclude that atomic displacements in *R*3*m* shall lower its enthalpy by transforming barrierlessly to a metastable state which will have another space group. Moreover, the *R*3*m* structure has a very high positive formation enthalpy of 0.819 eV/atom (endothermic Mo(s) + N_2(g) = MoN_2(s) reaction), while, in other transition metal nitrides, the ground-state structures usually have negative formation enthalpies, and even for high-pressure pernitrides the positive formation enthalpies at zero pressure are much lower (ΔH_f < 0.64 eV/atom, Table S2). The thermodynamic, dynamical, and mechanical instabilities of layered *R*3*m* MoN_2 motivated us to search for other possible ground-state structures at both atmospheric and high pressures. While the use of vdW-D2 correction is shown to be crucial to describe the structural properties of layered compounds, we show that the experimental bond lengths in bulk Mo_2N and MoN are well reproduced at the GGA-PBE level of theory; therefore, we still used the GGA-PBE level of theory for all bulk Mo−N based structures.

3.2. NiAs-Type MoN_2 Pernitride and Other Metastable Structures at Ambient Pressure. We started to perform fixed-composition structure searches at ambient pressure. The 12 predicted structures with lowest energies are shown in Figure 2. Almost all of the pernitride structures which contain discrete N_2 units (1−6) lie lower in energy than the structures

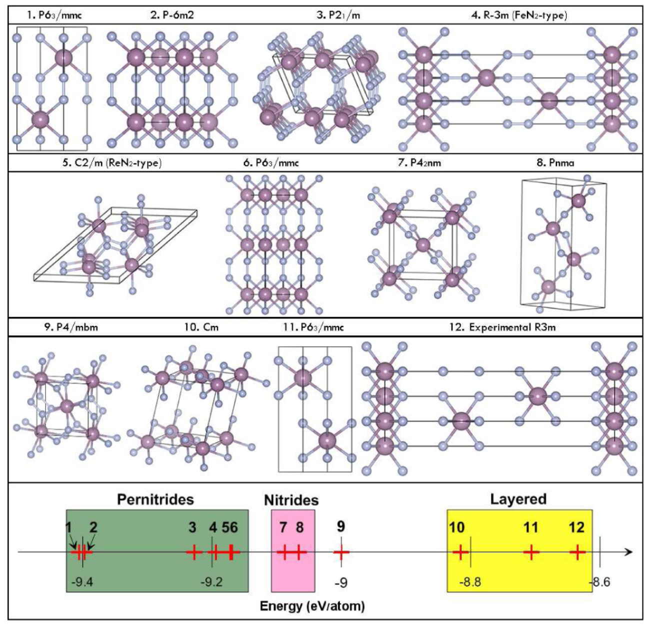

Figure 2. Predicted stable and metastable MoN_2 structures and their corresponding energies.

with isolated nitrogen anions (7−8) and the ones with layered structures (10−12). The lowest pernitride (N_2^{x-}, x = 2−4) is more stable by at least 0.34 eV/atom than the dinitrides ($2N^{3-}$). The energetic preference of the pernitride over the dinitride could be related to (i) covalent N−N bonds being more energetic than Mo−Mo and Mo−N ones and (ii) the high Mo oxidation state (VI) in the latter, as proposed for other transition metal MN_2 phases (FeN_2,[36] ReN_2[37]). Mo(VI) can only be found in solid-state extended structures under extremely oxidizing conditions such as in MoO_3 and polymolybdates.[38] In addition, the three van der Waals-type structures, *Cm*, $P6_3/mmc$, and *R*3*m* (10−12), are by far the less stable ones in our predicted MoN_2 structures (ΔH > 0.6 eV/atom). This result confirms that *R*3*m* MoN_2 is definitively not a viable structure. Recently, Wu et al.[39] proposed a nonmagnetic 2D T-type MoN_2 structure which contains octahedral Mo atoms. Our evolutionary searches locate the corresponding 3D T-type phase (space group *C*2/*m*) at 0.701 eV/atom higher in energy than the ground-state one. Its fully relaxed structure is reported in Figure S1. Moreover, its phonon dispersion curves present strong imaginary frequencies; thus, this octahedral Mo-containing layered structure is dynamically unstable.

At atmospheric pressure, the lowest-energy MoN_2 phase adopts a NiAs-type hexagonal structure ($P6_3/mmc$, if one considers N_2 groups as a single entity, Figure 3a). Its calculated phonon spectrum is shown in Figure S2. There are no imaginary phonon frequencies in the whole Brillion zone,

DOI: 10.1021/acs.jpcc.6b00665
J. Phys. Chem. C 2016, 120, 11060−11067

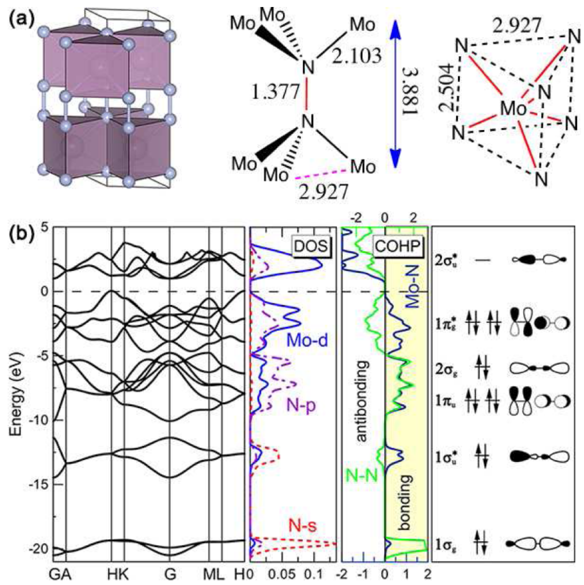

Figure 3. (a) Crystal structures of the ground-state $P6_3/mmc$ MoN_2. (b) The corresponding band structure, DOS, and −COHP plots computed at 0 GPa. The right part shows a schematic molecular orbital energy level diagram of N_2^{4-} unit.

which confirms its dynamical stability. This hexagonal $P6_3/mmc$ structure may also be described as stacking of the MoS_2-type MoN_2 sheets formed by N−Mo−N sandwiches (Mo−N = 2.103 Å; Mo−Mo = 2.927 Å). These MoN_2 sheets exhibit an AB stacking sequence but layers are bound not by weak van der Waals interactions as found in MoS_2-type structures. They are linked to each other through covalent N−N bonds. Thus, $P6_3/mmc$ MoN_2 contains discrete N_2 units, and is a transition metal pernitride. The molecular axis of N_2 is oriented parallel to the *c* axis, and the shortest N_2−N_2 separation is 2.504 Å.

The calculated N−N distance of 1.377 Å is close to the value found in N_2H_4 (1.45 Å) and PtN_2 (1.41 Å) but much longer than that in N_2F_2 (1.21 Å) and BaN_2 (1.23 Å) where a formal N═N double bond is assigned. Therefore, one may assign to the dinitrogen unit a formal charge of −4 leading to the singly bonded N_2^{4-} diatomic species. With fourteen valence electrons N_2^{4-} would be isoelectronic with F_2 (1.412 Å) and disulfide anion (S_2^{2-}), which is found in pyrite FeS_2 with four electrons in the antibonding $1\pi_g$* orbitals. Formally, one could assign MoN_2 as $Mo^{4+}(N_2^{4-})$, i.e., Mo is a d^2 metal, in agreement with the experimental results of Wang et al.[20] They noticed "the determined valence state for Mo is +3.5..., inferring a peculiar $4d^{2.5}$ electronic structure."

To confirm these electron counting and oxidation state assignments, the electronic properties of $P6_3/mmc$ MoN_2 were analyzed (Figure 3). Band structure and the density of states (DOS) show that the $P6_3/mmc$ phase is a semiconductor. Around −20 eV, the lowest states are dominated by N-2s states and correspond mainly to the bonding $1\sigma_g$ orbitals of diatomic N_2 units (see the molecular orbital interaction diagram of N_2^{4-} in Figure S3). Between −12 and −14 eV, the states are the nonbonding out-of-phase $1\sigma_u$ orbitals, which interact strongly with d orbitals. Below the Fermi level, the states are dominated by strong orbital mixing between $4d_{Mo}$ and $2p_N$ orbitals. Notice that the $2p_N$ states located between −5 eV and the Fermi level are occupied and the associated crystal orbitals possess N−N antibonding character. They correspond to the occupied $1\pi_g$* levels of the 14 electron diatomic N_2^{4-} species.

As mentioned previously, the formulation of $Mo^{4+}N_2^{4-}$ refers to a d^2 electron count for molybdenum atoms located in a trigonal prismatic coordination environment. According to crystal field theory, in a low-spin configuration—strong field ligands—these two d electrons occupy the d_{z^2} orbital while the four remaining d orbitals must be empty and higher in energy (Figure S4). Because pernitride $P6_3/mmc$ MoN_2 has a filled d_{z^2} band and unfilled $d_{xy}/d_{x^2-y^2}$ bands, MoN_2 should be a semiconductor, consistent with an energy gap found at the Fermi level (DOS, indirect gap, Figure 3). Moreover, an analysis of the chemical bonding between Mo and N in the crystal orbital Hamilton population (COHP) plots displayed in Figure 3 shows that all bonding levels have been filled with electrons, and all Mo−N antibonding states show up in the unoccupied crystal orbitals, well above the Fermi level. With respect to Mo−N bonding and to the octet rule for N_2^{4-}, $P6_3/mmc$ pernitride structure is ideal.

Even though the formation enthalpy of $P6_3/mmc$ MoN_2 is negative at 0 K and ambient pressure (ΔH_f = −0.297 eV/atom), this criterion is not sufficient to claim that the $P6_3/mmc$ pernitride phase is thermodynamically stable. In fact, a thermodynamically stable compound must be more stable than any isochemical mixture of the elements or other Mo_xN_y stoichiometries at a given pressure. A truly stable structure must lie on the convex hull constructed on the plot of the formation enthalpy versus composition $x = N/(N + Mo)$. For all possible phases of the Mo−N system, we generated the Mo−N convex hulls by using the variable-composition evolutionary algorithm combined with first-principles calculations and the results are shown in Figure 4. Formation enthalpies per atom of the Mo_xN_y phases are calculated with respect to elemental molybdenum and nitrogen in their most stable phases.

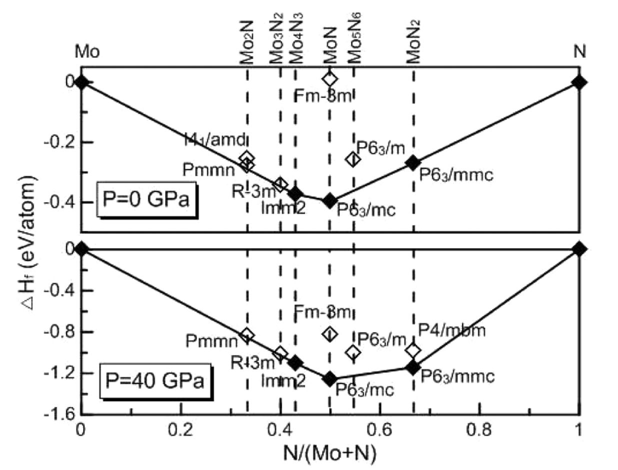

Figure 4. Convex hull diagrams of the Mo−N system at 0 and 40 GPa considering zero-point energy correction (solid squares, stable; open squares, metastable).

One may clearly see that, at both atmospheric pressure and 40 GPa, $P6_3/mmc$ MoN_2 lies on the convex hull. Therefore, pernitride MoN_2 is a truly stable structure, stable against decomposition into its elements and other Mo_xN_y phases at both ambient and high-pressure conditions. Our predicted pernitride phase should stimulate experimentalists to look for its synthesis and characterization. Besides MoN_2 and the experimentally well-known $P6_3$/mc-MoN, we also found a stable compound Mo_4N_3 which crystallizes in the *Imm*2 symmetry, while Mo_2N, Mo_3N_2, and Mo_5N_6 are metastable in the whole studied pressure range (Table S3 and Figure S5).

3.3. Pressure Effect on MoN_2. As transition metal nitrides are usually experimentally obtained under high pressure, we studied the relative enthalpies of different MoN_2 structures compared with the experimental claimed $R3m$ structure as a function of pressure. For comparison, the structures discussed in MoS_2-type ($P6_3/mmc$), OsN_2-type ($P6/mmm$),[18] Cm, and ReN_2-type ($C2/m$)[37] were considered in our study. The thermodynamic stability of MoN_2 with respect to decomposition into elemental Mo + N_2 and reactants MoN + $^1/_2N_2$ was also discussed. The body-centered-cubic Mo ($Im\overline{3}m$), hexagonal MoN ($P6_3$/mc),[40] and depending on the applied pressures, α, $P4_12_12$, cg phases of N[22,41] were chosen as reference states.

It is seen from Figure 5 that $P6_3/mmc$ pernitride is thermodynamically stable against decomposition into the

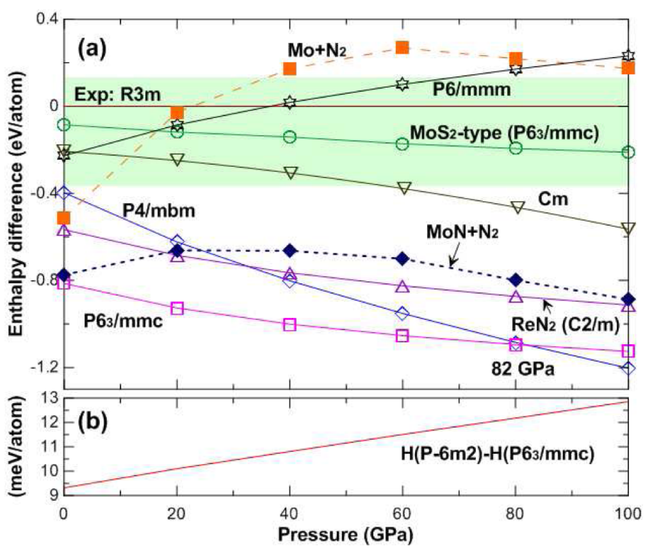

Figure 5. (a) The calculated enthalpy differences of various MoN_2 structures relative to the claimed $R3m$ structure as a function of pressure together with decomposition into the mixture of Mo + N_2 and MoN + $^1/_2N_2$. (b) Energy difference of $P\overline{6}m2$ and $P6_3/mmc$ structures as a function of pressure.

mixture of Mo + N_2 or MoN + $^1/_2N_2$ over the whole pressure range. The experimental $R3m$ MoN_2 is thermodynamically unstable with respect to decomposition into Mo + N_2 below roughly 20 GPa. Moreover, it is seen that, for all phases with layered structures ($P6/mmm$, MoS_2-type $P6_3/mmc$, Cm, and $R3m$), their formation enthalpies are positive below 10 GPa and become negative under high pressure. However, they all have much higher enthalpies than our $P6_3/mmc$ pernitride phase and the MoN + $^1/_2N_2$ reactants over the whole pressure range, indicating their chemical instability. It is noteworthy that we also found a WN_2-type ($P\overline{6}m2$)[42] structure with enthalpy only 9 meV/atom higher at ambient pressure and 13 meV/atom at 100 GPa than the $P6_3/mmc$ MoN_2. Also, our calculations show that the fully optimized $R3m$ MoN_2 structure is nonmagnetic, thus considering the magnetic corrections will not affect the relative stability of MoN_2 (Table S1).

Previous studies proposed that the $P6/mmm$ structure is a universal ground-state structure for all MN_2 compounds at low pressures (M = Os, Ir, Ru, and Rh),[18] a statement that could not be applied for the MoN_2 system. Nevertheless, MoN_2 adopts the same tetragonal $P4/mbm$ structure proposed for these nitrides at high pressures, and it can be obtained through the phase transformation via the marcasite structure.[18] Starting from ambient pressure, the NiAs-type $P6_3/mmc$ structure remains competitive up to 82 GPa. Above, we found the tetragonal $P4/mbm$ structure as a ground state (Figure 5). The calculated phonon spectrum of the predicted $P4/mbm$ MoN_2 confirms its dynamical stability (Figure S2). The crystal structure of $P4/mbm$ MoN_2 is shown in Figure 6. The $P4/$

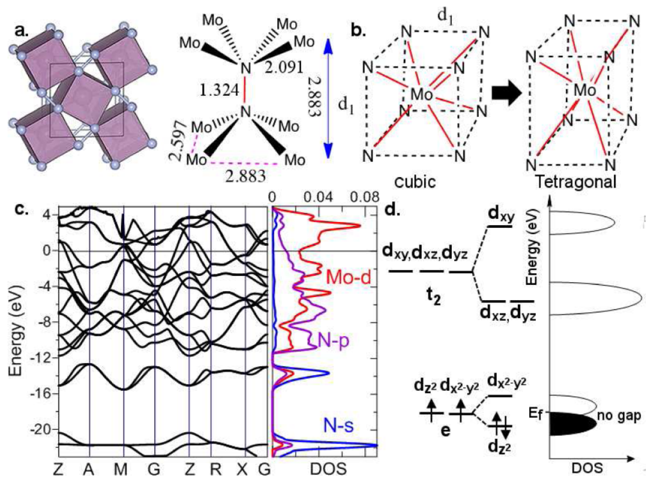

Figure 6. (a) Crystal structure of $P4/mbm$ MoN_2 at 100 GPa. (b) Jahn−Teller elongation of the MoN_8 cuboids. (c) Band structure and DOS of $P4/mbm$ MoN_2 at 100 GPa. (d) A schematic explanation of the crystal field splitting of the d_{Mo} orbital.

mbm phase contains MoN_8 edge-sharing cuboids stacking along the c axis with a Mo−N bond length of 2.091 Å at 100 GPa. Here we have N_2 dumbbells encapsulated in the slightly elongated Mo_8 cube. The N−N bond length is calculated at 1.324 Å at 100 GPa and 1.369 Å at atmospheric pressure, a value close to the one discovered in the $P6_3/mmc$ structure (1.377 Å at 0 GPa). Thus, the singly bonded N_2 unit remains and the $P4/mbm$ phase is also a pernitride structure.

The structural features of the $P4/mbm$ MoN_2 are mirrored in the electronic properties, shown in Figure 6. As DOS in the pernitride $P6_3/mmc$ phase, N_2 states are clearly identified in $P4/mbm$ DOS: $1\sigma_g$ around −22 eV, $1\sigma_u{}^*$ at −14 eV, $1\pi_u$ levels between −7 and −11 eV, $2\sigma_g$ between −5 and −7 eV, and the fully occupied $1\pi_g{}^*$ located above the Fermi level. Consequently, for electron counting purposes, the dinitrogen unit should be formally considered as $N_2{}^{4-}$, a pernitride unit isoelectronic to F_2 molecules. Its electronic ground-state configuration is $(1\sigma_g)^2(1\sigma_u{}^*)^2(1\pi_u)^4(2\sigma_g)^2(1\pi_g{}^*)^4$ for 14 valence electrons, and its bond order is one (Figure S3). Note that the discrete N_2 units point directly toward the square faces of the eight-coordinate polyhedra of the molybdenum atoms (Mo−N bonding length is 2.091 Å at 100 GPa) and are perpendicular to each other in order to minimize the steric repulsion between the nitrogen σ-lone pairs (Pauli repulsions). Formally, this leaves the molybdenum atoms of MoN_2 in a d^2 configuration (Mo^{4+}). In a cubic crystal field, the five d orbitals split into doubly degenerate levels, e(d_{z^2}, $d_{x^2-y^2}$) and triply degenerate ones, t_2(d_{xy}, d_{xz}, d_{yz}), leading to half-filled e levels.

This degenerate electronic configuration e^2 is Jahn−Teller unstable: the cubic MoN_8 complexes should undergo a geometric distortion to remove this degeneracy. Effectively, a

DOI: 10.1021/acs.jpcc.6b00665
J. Phys. Chem. C 2016, 120, 11060−11067

weak Jahn−Teller effect is observed in the *P*4/*mbm* phase (Figure 6b) with the N−N distances in tetragonal MoN_8 units 2.330 and 2.597 Å at 100 GPa. As the Jahn−Teller effect is very weak for a low-spin d^2 configuration, a small $d_{z^2}/d_{x^2-y^2}$ splitting occurs (Figure 6d). Nevertheless, the tetragonal *P*4/*mbm* phase is expected to be a metal due to the overlap of the filled d_{z^2} and unfilled $d_{x^2-y^2}$ bands, as confirmed by the calculated DOS (Figure 6c). Moreover, the covalent nature of the bonding is manifested by the significant penetration of the metal d levels into the nitrogen p block, and the Mo−N bonding states are all fully occupied while the antibonding ones are unoccupied. This electronic situation explains well the stability of ground-state *P*4/*mbm* under high pressure.

3.4. Mechanical Properties. The mechanical properties of the MoN_2 structures were further studied. The calculated elastic constants C_{ij}, bulk modulus B, shear modulus G, and Young's modulus E are presented in Table 2. We noticed that the calculated elastic constants of $P6_3/mmc$ and *P*4/*mbm* structures satisfy the mechanical stability criteria.[28] Furthermore, $P6_3/mmc$ MoN_2 possesses a remarkably high C_{33} value (952 GPa) which is comparable to diamond (C_{33} = 1079 GPa[43]), revealing its extremely high stiffness along the *c* axis, which could be well understood by the strong directional Mo−N and N−N covalent bonds along the *c* axis. On the basis of the Voigt−Reuss−Hill (VRH) approximation,[44−46] the calculated B and G of $P6_3/mmc$ MoN_2 are 338 and 206 GPa, respectively, comparable to OsN_2 (B = 353 GPa and G = 222 GPa) and IrN_2 (B = 333 GPa and G = 205 GPa).[37] The high-pressure *P*4/*mbm* structure has a comparable bulk modulus (B = 345 GPa) but exhibits a much larger shear modulus (G = 251 GPa) than OsN_2 and IrN_2.

Figure 7 illustrates the directional dependence of Young's modulus for the two novel MoN_2 structures. The degree of deviation of its shape from spherical indicates the degree of anisotropy. From Figure 7, one can find that the $P6_3/mmc$ structure is much more anisotropic than the *P*4/*mbm* structure, due to the N−Mo−N sandwich stacking and strong directional Mo−N and N−N covalent bonds along the *c* direction (large C_{33}). For tetragonal *P*4/*mbm* MoN_2, the comparable C_{11}, C_{22}, and C_{33} make Young's modulus more isotropic, consistent with the atomic arrangements in the two novel structures. Moreover, the Poisson's ratios υ for $P6_3/mmc$ and *P*4/*mbm* structures are 0.247 and 0.207, respectively, close to 0.2. A low Poisson's ratio results from directional bonds, which increases the shear modulus and limits the motion of dislocations, thereby increasing the material's hardness. The theoretical Vickers hardness H_v was estimated by using Chen's model,[47] H_v = $2(\kappa^2 G)^{0.585} - 3$. The estimated hardness values for $P6_3/mmc$ and *P*4/*mbm* structures are 22.3 and 32 GPa, respectively, making them potentially interesting for applications as hard coating materials.

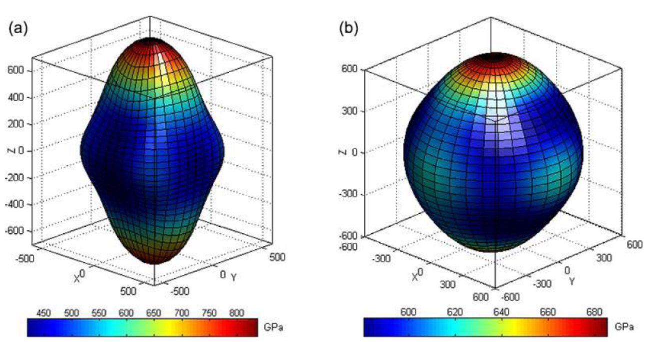

Figure 7. Directional dependence of the Young's modulus for MoN_2 at ambient pressure: (a) $P6_3/mmc$; (b) *P*4/*mbm*.

4. CONCLUSION

In summary, we have found that the experimentally proposed MoS_2-type MoN_2 structure is unstable, as indicated by the negative C_{44} value, imaginary phonon frequencies, and positive enthalpy of formation based on first-principles calculations. By using the evolutionary methodology USPEX for crystal structure prediction, we have extensively explored the potentially stable structures of MoN_2 in the pressure range 0−100 GPa. Two energetically more stable pernitride phases were discovered. Enthalpy calculations demonstrate that the hexagonal $P6_3/mmc$ MoN_2 will transform into a tetragonal *P*4/*mbm* structure above 82 GPa. The $P6_3/mmc$ phase is a narrow-gap semiconductor, while the high-pressure *P*4/*mbm* structure is metallic. Both pernitride MoN_2 structures are mechanically and dynamically stable. The atmospheric ground-state structure has a high bulk modulus (B = 338 GPa) and shear modulus (G = 206 GPa), and is predicted to be a hard material. Further chemical bonding analyses reveal that the two MoN_2 structures incorporate a tetravalent metal (Mo^{4+}, d^2) and a N_2^{4-} species with a covalent N−N single bond.

■ ASSOCIATED CONTENT

Supporting Information

The Supporting Information is available free of charge on the ACS Publications website at DOI: 10.1021/acs.jpcc.6b00665.

Calculated structural parameters, formation enthalpies, and magnetic properties of the stable and metastable Mo−N structures at selected pressures; phonon dispersion curves and ICOHP values of the predicted $P6_3/mmc$ and *P*4/*mbm* MoN_2; molecular orbital diagram of N_2^{4-} unit; crystal field splitting of the d_{Mo} levels in the $P6_3/mmc$ MoN_2; crystal structure of *C*2/*m* MoN_2; computed XRD patterns of ground state MoN_2 structures (PDF)

■ AUTHOR INFORMATION

Corresponding Authors

*E-mail: yushuyin2014@gmail.com.
*E-mail: gilles.frapper@univ-poitiers.fr.

Author Contributions

The manuscript was written through contributions of all authors. All authors have given approval to the final version of the manuscript.

Notes

The authors declare no competing financial interest.

■ ACKNOWLEDGMENTS

This work was supported by the Natural Science Foundation of China (No. 51372203, 51332004 and DMR-1231586), the Foreign Talents Introduction and Academic Exchange Program of China (No. B08040), the Fundamental Research Funds for the Central Universities in China (No. 3102015BJ(II)JGZ005), the MIPT internship program supported by the Government of Russian Federation (No. 14.A12.31.0003 and top-5-100 grant to MIPT), the GDRI RFCCT CNRS (DNM-evol program) and the Hubert Curien Partnerships PHC XU GUANGQI

2015 (No. 34455PE) part of the French Ministry of Foreign Affairs, the Région Poitou-Charentes (France) for a Ph.D. fellowship. The authors also acknowledge the high performance computing center of NWPU and mesocentre de calculs de Poitou Charentes at Université de Poitiers for the allocation of computing time on their machines.

REFERENCES

(1) Hägg, G. The Iron-Nitrogen System. *Nova Acta Reg. Soc. Sci. Upsaliensis* **1928**, *4*, 1.

(2) Hägg, G. X-Ray Diffraction Investigations on Molybdenum and Tungsten Nitrides. *Z. Phys. Chem. B* **1930**, *7*, 339−362.

(3) Brese, N. E.; O'Keeffe, M. Crystal Chemistry of Inorganic Nitrides. *Complexes, Clusters and Crystal Chemistry*; Springer: Berlin Heidelberg, 1992; pp 307−308.

(4) Toth, L. *Transition Metal Carbides and Nitrides*; Elsevier: Academic Press, 2014, pp 12069−12073.

(5) Birkholz, M.; Ehwald, E. K.; Kulse, P.; Drews, J.; Fröhlich, M.; Haak, U.; Kaynak, M.; Matthus, E.; Schulz, K.; Wolansky, D. Ultrathin Tin Membranes as a Technology Platform for CMOS-Integrated MEMS and BioMEMS Devices. *Adv. Funct. Mater.* **2011**, *21*, 1652−1656.

(6) Hintermann, H. E. Tribological and Protective Coatings by Chemical Vapour Deposition. *Thin Solid Films* **1981**, *84*, 215−243.

(7) Wang, S.; Antonio, D.; Yu, X.; Zhang, J.; Cornelius, A. L.; He, D.; Zhao, Y. The Hardest Superconducting Metal Nitride. *Sci. Rep.* **2015**, *5*, 13733.

(8) Zerr, A.; Miehe, G.; Riedel, R. Synthesis of Cubic Zirconium and Hafnium Nitride Having Th_3P_4 Structure. *Nat. Mater.* **2003**, *2*, 185−189.

(9) Salamat, A.; Hector, A. L.; Gray, B. M.; Kimber, S. A. J.; Bouvier, P.; Mcmillan, P. F. Synthesis of Tetragonal and Orthorhombic Polymorphs of Hf_3N_4 by High-Pressure Annealing of a Prestructured Nanocrystalline Precursor. *J. Am. Chem. Soc.* **2013**, *135*, 9503−9511.

(10) Salamat, A.; Woodhead, K.; Shah, S. I. U.; Hector, A. L.; McMillan, P. F. Synthesis of U_3Se_5 and U_3Te_5 Type Polymorphs of Ta_3N_5 by Combining High Pressure-Temperature Pathways with a Chemical Precursor Approach. *Chem. Commun.* **2014**, *50*, 10041−10044.

(11) Zerr, A.; Miehe, G.; Li, J. W.; Dzivenko, D. A.; Bulatov, V. K.; Höfer, H.; Bolfan Casanova, N.; Fialin, M.; Brey, G.; Watanabe, T. High-Pressure Synthesis of Tantalum Nitride Having Orthorhombic U_2S_3 Structure. *Adv. Funct. Mater.* **2009**, *19*, 2282−2288.

(12) Wang, S. M.; Yu, X. H.; Lin, Z. J.; Zhang, R. F.; He, D. W.; Qin, J. Q.; Zhu, J. L.; Han, J. T.; Wang, L.; Mao, H. k. Synthesis, Crystal Structure, and Elastic Properties of Novel Tungsten Nitrides. *Chem. Mater.* **2012**, *24*, 3023−3028.

(13) Salamat, A.; Hector, A. L.; Kroll, P.; McMillan, P. F. Nitrogen-Rich Transition Metal Nitrides. *Coord. Chem. Rev.* **2013**, *257*, 2063−2072.

(14) Crowhurst, J. C.; Goncharov, A. F.; Sadigh, B.; Evans, C. L.; Morrall, P. G.; Ferreira, J. L.; Nelson, A. J. Synthesis and Characterization of the Nitrides of Platinum and Iridium. *Science* **2006**, *311*, 1275−1278.

(15) Gregoryanz, E.; Sanloup, C.; Somayazulu, M.; Badro, J.; Fiquet, G.; Mao, H. K.; Hemley, R. J. Synthesis and Characterization of a Binary Noble Metal Nitride. *Nat. Mater.* **2004**, *3*, 294−297.

(16) Crowhurst, J. C.; Goncharov, A. F.; Sadigh, B.; Zaug, J.; Aberg, D.; Meng, Y.; Prakapenka, V. B. Synthesis and Characterization of Nitrides of Iridium and Palladium. *J. Mater. Res.* **2008**, *23*, 1−5.

(17) Young, A. F.; Sanloup, C.; Gregoryanz, E.; Scandolo, S.; Hemley, R. J.; Mao, H. k. Synthesis of Novel Transition Metal Nitrides IrN_2 and OsN_2. *Phys. Rev. Lett.* **2006**, *96*, 155501.

(18) Li, Y. W.; Wang, H.; Li, Q.; Ma, Y. M.; Cui, T.; Zou, G. T. Twofold Coordinated Ground-State and Eightfold High-Pressure Phases of Heavy Transition Metal Nitrides MN_2 (M= Os, Ir, Ru, and Rh). *Inorg. Chem.* **2009**, *48*, 9904−9909.

(19) Niwa, K.; Suzuki, K.; Muto, S.; Tatsumi, K.; Soda, K.; Kikegawa, T.; Hasegawa, M. Discovery of the Last Remaining Binary Platinum-Group Pernitride RuN_2. *Chem. - Eur. J.* **2014**, *20*, 13885−13888.

(20) Wang, S. M.; Ge, H.; Sun, S. L.; Zhang, J. Z.; Liu, F. M.; Wen, X. D.; Yu, X. H.; Wang, L. P.; Zhang, Y.; Xu, H. W. A New Molybdenum Nitride Catalyst with Rhombohedral MoS_2 Structure for Hydrogenation Applications. *J. Am. Chem. Soc.* **2015**, *137*, 4815−4822.

(21) Frapper, G.; Pélissier, M.; Hafner, J. CO Adsorption on Molybdenum Nitride's γ-Mo_2N (100) Surface: Formation of NCO Species? A Density Functional Study. *J. Phys. Chem. B* **2000**, *104*, 11972−11976.

(22) Oganov, A. R.; Glass, C. W. Crystal Structure Prediction Using *Ab* Initio Evolutionary Techniques: Principles and Applications. *J. Chem. Phys.* **2006**, *124*, 244704.

(23) Oganov, A. R.; Ma, Y. M.; Lyakhov, A. O.; Valle, M.; Gatti, C. Evolutionary Crystal Structure Prediction as a Method for the Discovery of Minerals and Materials. *Rev. Mineral. Geochem.* **2010**, *71*, 271−298.

(24) Oganov, A. R.; Lyakhov, A. O.; Valle, M. How Evolutionary Crystal Structure Prediction Works and Why? *Acc. Chem. Res.* **2011**, *44*, 227−237.

(25) Kresse, G.; Furthmüller, J. Efficient Iterative Schemes for *Ab* Initio Total-Energy Calculations Using a Plane-Wave Basis Set. *Phys. Rev. B: Condens. Matter Mater. Phys.* **1996**, *54*, 11169−11186.

(26) Liu, G.; Liu, S. B.; Xu, B.; Ouyang, C. Y.; Song, H. Y. Generalized Gradient Approximation Made Simple. *J. Appl. Phys.* **2015**, *112*, 666.

(27) Togo, A.; Oba, F.; Tanaka, I. First-Principles Calculations of the Ferroelastic Transition between Rutile-Type and $CaCl_2$-Type SiO_2 at High Pressures. *Phys. Rev. B: Condens. Matter Mater. Phys.* **2008**, *78*, 134106.

(28) Born, M.; Huang, K. *Dynamical Theory of Crystal Lattices.* Clarendon Press: Oxford, 1954, pp 104−113.

(29) Dronskowski, R.; Bloechl, P. E. Crystal Orbital Hamilton Populations (COHP): Energy-Resolved Visualization of Chemical Bonding in Solids Based on Density-Functional Calculations. *J. Phys. Chem.* **1993**, *97*, 8617−8624.

(30) Deringer, V. L.; Tchougréeff, A. L.; Dronskowski, R. Crystal Orbital Hamilton Population (COHP) Analysis as Projected from Plane-Wave Basis Sets. *J. Phys. Chem. A* **2011**, *115*, 5461−6.

(31) Maintz, S.; Deringer, V. L.; Tchougréeff, A. L.; Dronskowski, R. Analytic Projection from Plane-Wave and Paw Wavefunctions and Application to Chemical-Bonding Analysis in Solids. *J. Comput. Chem.* **2013**, *34*, 2557−2567.

(32) Wu, F.; Huang, C.; Wu, H.; Lee, C.; Deng, K.; Kan, E.; Jena, P. Atomically Thin Transition-Metal Dinitrides: High-Temperature Ferromagnetism and Half-Metallicity. *Nano Lett.* **2015**, *15*, 8277−8281.

(33) van Mourik, T.; Gdanitz, R. J. A Critical Note on Density Functional Theory Studies on Rare-Gas Dimers. *J. Chem. Phys.* **2002**, *116*, 9620−9623.

(34) Langreth, D. C.; Dion, M.; Rydberg, H.; Schröder, E.; Hyldgaard, P.; Lundqvist, B. I. Van Der Waals Density Functional Theory with Applications. *Int. J. Quantum Chem.* **2005**, *101*, 599−610.

(35) Grimme, S. Semiempirical GGA-Type Density Functional Constructed with a Long-Range Dispersion Correction. *J. Comput. Chem.* **2006**, *27*, 1787−1799.

(36) Michael, W.; Dronskowski, R. A New Phase in the Binary Iron Nitrogen System? The Prediction of Iron Pernitride, FeN_2. *Chem. - Eur. J.* **2011**, *17*, 2598−603.

(37) Wang, Y. C.; Yao, T. K.; Yao, J. L.; Zhang, J. W.; Gou, H. Y. Does the Real ReN_2 Have the MoS_2 Structure? *Phys. Chem. Chem. Phys.* **2013**, *15*, 183−187.

(38) Cotton, F. A.; Wing, R. M. Properties of Metal-to-Oxygen Multiple Bonds, Especially Molybdenum-to-Oxygen Bonds. *Inorg. Chem.* **1965**, *4*, 867−873.

(39) Wu, H. P.; Qian, Y.; Lu, R. F.; Tan, W. S. A Theoretical Study on the Electronic Property of a New Two-Dimensional Material Molybdenum Dinitride. *Phys. Lett. A* **2016**, *380*, 768−772.

(40) Belonoshko, A. B.; Burakovsky, L.; Chen, S. P.; Johansson, B.; Mikhaylushkin, A. S.; Preston, D. L.; Simak, S. I.; Swift, D. C. Molybdenum at High Pressure and Temperature: Melting from Another Solid Phase. *Phys. Rev. Lett.* **2008**, *100*, 135701−135701.
(41) Pickard, C. J.; Needs, R. J. High-Pressure Phases of Nitrogen. *Phys. Rev. Lett.* **2009**, *102*, 125702.
(42) Wang, H.; Li, Q.; Li, Y. W.; Xu, Y.; Cui, T.; Oganov, A. R.; Ma, Y. M. Ultra-Incompressible Phases of Tungsten Dinitride Predicted from First Principles. *Phys. Rev. B: Condens. Matter Mater. Phys.* **2009**, *79*, 132109.
(43) Mcskimin, H. J. Elastic Moduli of Diamond as a Function of Pressure and Temperature. *J. Appl. Phys.* **1972**, *43*, 2944−2948.
(44) Voigt, W. *Lehrbuch Der Kristallphysik*; Benedictus Gotthelf Teubher: Leipzig 1928, p 739.
(45) Hill, R. The Elastic Behaviour of a Crystalline Aggregate. *Proc. Phys. Soc., London, Sect. A* **1952**, *65*, 349−354.
(46) Chandrasekar, S.; Santhanam, S. A Calculation of the Bulk Modulus of Polycrystalline Materials. *J. Mater. Sci.* **1989**, *24*, 4265−4267.
(47) Chen, X. Q.; Niu, H. Y.; Li, D. Z.; Li, Y. Y. Modeling Hardness of Polycrystalline Materials and Bulk Metallic Glasses. *Intermetallics* **2011**, *19*, 1275−1281.

DOI: 10.1021/acs.jpcc.6b00665
J. Phys. Chem. C 2016, 120, 11060−11067